

Silencing the Menkes Copper-Transporting ATPase (*Atp7a*) Gene in Rat Intestinal Epithelial (IEC-6) Cells Increases Iron Flux via Transcriptional Induction of Ferroportin 1 (*Fpn1*)^{1–3}

Sukru Gulec and James F. Collins*

Food Science and Human Nutrition Department, University of Florida, Gainesville, FL

Abstract

The Menkes copper-transporting ATPase (*Atp7a*) gene is induced in rat duodenum during iron deficiency, consistent with copper accumulation in the intestinal mucosa and liver. To test the hypothesis that ATP7A influences intestinal iron metabolism, the *Atp7a* gene was silenced in rat intestinal epithelial (IEC-6) cells using short hairpin RNA (shRNA) technology. Perturbations in intracellular copper homeostasis were noted in knockdown cells, consistent with the dual roles of ATP7A in pumping copper into the *trans*-Golgi (for cuproenzyme synthesis) and exporting copper from cells. Intracellular iron concentrations were unaffected by *Atp7a* knockdown. Unexpectedly, however, vectorial iron (⁵⁹Fe) transport increased (~33%) in knockdown cells grown in bicameral inserts and increased further (~70%) by iron deprivation (compared with negative control shRNA-transfected cells). Additional experiments were designed to elucidate the molecular mechanism of increased transepithelial iron flux. Enhanced iron uptake by knockdown cells was associated with increased expression of a ferrireductase (duodenal cytochrome b) and activity of a cell-surface ferrireductase. Increased iron efflux from knockdown cells was likely mediated via transcriptional activation of the ferroportin 1 gene (by an unknown mechanism). Moreover, *Atp7a* knockdown significantly attenuated expression of an iron oxidase [hephaestin (HEPH); by ~80%] and membrane ferroxidase activity (by ~50%). Cytosolic ferroxidase activity, however, was retained in knockdown cells (75% of control cells), perhaps compensating for diminished HEPH activity. This investigation has thus documented alterations in iron homeostasis associated with *Atp7a* knockdown in enterocyte-like cells. Alterations in copper transport, trafficking, or distribution may underlie the increase in transepithelial iron flux noted when ATP7A activity is diminished. *J. Nutr.* 144: 12–19, 2014.

Introduction

Iron is an essential trace mineral involved in a variety of physiologic pathways and disease processes. Excess iron is toxic in biologic systems given its propensity to mediate production of reactive oxygen species (ROS)⁴, so iron concentrations are tightly

controlled (1). In mammals, this is achieved by precise regulation of iron absorption in the proximal small bowel, because no active excretory mechanisms exist. Intestinal iron transport is inhibited when body iron stores are high and is enhanced by iron deprivation. During iron overload, vectorial iron flux is blocked by a liver-derived peptide hormone, hepcidin, which interacts with the iron exporter ferroportin 1 (FPN1) on the basolateral surface of intestinal enterocytes, causing its internalization and degradation (2). When iron stores are low, hemoglobin concentrations fall and tissue hypoxia ensues, including in the duodenal epithelium. This triggers transcriptional induction of genes encoding iron transport-related proteins by a hypoxia-inducible *trans*-acting factor [hypoxia-inducible factor 2 α (HIF2 α)] (3–5), leading to enhanced iron extraction from the diet. It was also noted that genes encoding copper homeostasis-related proteins were induced in the duodenal epithelium of iron-deprived rats (6,7), including intracellular copper-binding proteins (metallothionein I/II) and an intestinal copper exporter [Menkes

¹ Supported by NIH grant 1 R01 DK074867 (to J.F.C.).

² Author disclosures: S. Gulec and J. F. Collins, no conflicts of interest.

³ Supplemental Tables 1 and 2 are available from the "Online Supporting Material" link in the online posting of the article and from the same link in the online table of contents at <http://jn.nutrition.org>.

⁴ Abbreviations used: *Atp7a*, Menkes copper-transporting ATPase; *Atp7b*, Wilsons copper-transporting ATPase; *Cp*, ceruloplasmin; *Dcytb*, duodenal cytochrome b; DFO, deferoxamine; *Dmt1*, divalent metal transporter 1; FOX, ferroxidase; *Fpn1*, ferroportin 1; *Heph*, hephaestin; HIF2 α , hypoxia-inducible factor 2 α ; hnRNA, heteronuclear RNA; IEC-6, rat intestinal epithelial; *Mt1a*, metallothionein 1a; ROS, reactive oxygen species; shRNA, short hairpin RNA; TEER, transepithelial electrical resistance; *Tfr1*, transferrin receptor 1; TGN, *trans*-Golgi Network.

* To whom correspondence should be addressed. E-mail: jfcollins@ufl.edu.

copper-transporting ATPase (ATP7A)]. A subsequent investigation provided evidence that the *Atp7a* gene was transcriptionally regulated by HIF2 α during iron deficiency/hypoxia, demonstrating coregulation with iron transporters (8).

Tissue and serum copper concentrations increase in many mammalian species during iron deprivation (9–11). During iron deficiency, copper accumulates in the intestinal mucosa (12), liver, and serum of iron-deficient rats (7) and in serum of several mammalian species, including humans (13,14). Interestingly, enterocytes and hepatocytes are important for control of iron homeostasis, and the blood-borne multicopper ferroxidase, ceruloplasmin (CP), is critical for iron release from storage sites (15). Copper accumulation in duodenal enterocytes may enhance production of a copper-containing iron oxidase, hephaestin (HEPH), which functionally couples with FPN1 to promote iron efflux (16). In hepatocytes, where CP production occurs, increased copper concentrations may enhance biosynthesis of *holo*-CP, leading to increased concentrations of the active, circulating ferroxidase (FOX) (11). Copper may thus play an important role in the maintenance of iron homeostasis, and a detailed mechanistic understanding of how copper concentrations are controlled during perturbations in iron status is likely to provide novel insight into iron metabolism.

The current investigation sought to test the hypothesis that the ATP7A copper transporter expressed in duodenal enterocytes is important for control of intestinal iron transport. This postulate derives from the above-described alterations in tissue and serum copper concentrations during iron deficiency, the documented influence of the multicopper FOXs on iron homeostasis, and the functional role of ATP7A in copper homeostasis. ATP7A is the rate-limiting step in body copper acquisition (17) and could thus directly influence copper concentrations in duodenal enterocytes and hepatocytes, cells important for regulation of iron homeostasis. Moreover, ATP7A functions to pump copper into the *trans*-Golgi Network (TGN), probable sites of biosynthesis of the multicopper FOXs HEPH (in enterocytes) and CP (in hepatocytes). To test this hypothesis, *Atp7a* expression was effectively silenced in a commonly used model of the mammalian intestinal epithelium, rat intestinal epithelial (IEC-6) cells. These cells express an inducible iron transport system, reflecting *in vivo* regulation of iron absorption (18–22). This study showed that *Atp7a* knockdown in IEC-6 cells enhanced trans-epithelial iron flux via a novel molecular mechanism involving transcriptional induction of *Fpn1* gene expression.

Materials and Methods

Cell culture and development of *Atp7a* knockdown IEC-6 cells

IEC-6 cells were purchased from American Type Culture Collection and were maintained at 37°C in a 5% CO₂/95% O₂ environment in DMEM supplemented with 10% (v:v) FBS, 10 U/mL insulin, and antibiotics (100 U/mL penicillin and streptomycin). Short hairpin RNAs (shRNAs) targeting the rat *Atp7a* mRNA and a negative-control shRNA cloned into the block-iT vector were purchased from Invitrogen (sequences are shown in Supplemental Table 1). *Atp7a* knockdown cells were created by cotransfection with 3 shRNA-expressing plasmids followed by zeocine selection (250 μ g/mL; Invitrogen). Cells were subsequently maintained in regular medium plus zeocine. In all experiments, cells stably transfected with *Atp7a*-specific shRNA-expressing plasmids were compared with cells stably transfected with the negative-control shRNA-expressing plasmid. To test *Atp7a* knockdown at the functional level, cells were grown on 100-mm cell culture dishes, and upon confluence 100 μ mol/L CuCl₂ was added to the medium for 3 or 16 h. In some experiments, to mimic the iron-deficient condition, cells were treated with 200 μ mol/L deferoxamine (DFO; an iron chelator) for 24 h. Intracellular copper and iron concentrations were

measured by atomic absorption spectroscopy. Before experimentation, cells were routinely grown in cell culture-treated plastic dishes for ~8 d postconfluence to allow for differentiation (23–25). All experiments were conducted with cells between passages 15 and 25.

Iron transport studies

IEC-6 cells (100,000) were plated on 0.4- μ m pore-size collagen-coated trans-well inserts (Corning) in 12-well plates and allowed to grow for ~8 d postconfluence. Cell monolayer integrity was assessed by measuring transepithelial electric resistance (TEER) with an evom meter (World Precision Instruments). TEER of IEC-6 monolayers peaks at ~36–40 Ω \times cm² after 6–8 d postconfluence (24,25). Tight junction integrity was also assessed by phenol red flux (26). ⁵⁹Fe uptake into cells (transport) and efflux to the basolateral chamber (transfer) were determined by accepted methods (27,28). Briefly, cells were preincubated with Krebs-Ringer (uptake) buffer (130 mmol/L NaCl, 10 mmol/L KCl, 1 mmol/L MgSO₄, 5 mmol/L glucose, and 50 mmol/L HEPES; pH 7.0) in a cell culture incubator for 30 min at 37°C. After preincubation, TEER was measured to ensure that cells had tight gap junctions. Cells were then incubated with 0.5 μ mol/L ⁵⁹Fe-ferric citrate in uptake buffer for 90 min in a cell culture incubator at 37°C followed by rinsing 3 times with wash buffer (150 mmol/L NaCl₂, 10 mmol/L HEPES; pH 7.0; 1 mmol/L EDTA) to remove any surface-bound iron. Cell were then lysed with 0.2 N NaOH containing 0.2% SDS. Radioactivity was subsequently quantified in lysates and in transport buffer collected from the lower chamber by γ -counting. Protein concentrations of cell lysates were determined by a standard protein assay. Uptake and transfer of ⁵⁹Fe are expressed as counts per minute/mg of protein.

qRT-PCR

Total cellular and nuclear RNA was isolated with the use of Trizol reagent (Invitrogen). SYBR-Green qRT-PCR was performed according to a well-established protocol (29). Oligonucleotide primers were designed to span large introns to avoid amplification from genomic DNA. Standard curve reactions validated each primer pair, and melt curves routinely showed single amplicons. Expression of experimental genes was normalized to expression of cyclophilin, which did not vary significantly across samples. Mean fold changes in mRNA expression were calculated by using the 2^{- $\Delta\Delta$ C_t} analysis method (30). RNA samples for heteronuclear RNA (hnRNA) quantification were treated with DNase I (Ambion) to eliminate possible genomic DNA contamination. Primers for amplification of duodenal cytochrome b (*Dcytb*) and *Fpn1* hnRNA were designed to bind in exon 3 (forward) and at the exon 3–intron 3 boundary (reverse). Primer sequences are listed in Supplemental Table 2.

Protein isolation and immunoblotting

RIPA buffer [50 mmol/L Tris-HCl; pH 7.4; 150 mmol/L NaCl, 1% (v:v) NP-40, 0.1% (wt:v) SDS, 0.5% (wt:v) sodium deoxycholate] containing protease inhibitors was used to isolate total cellular proteins. Membrane and cytosolic proteins were isolated as described previously (31). Proteins were separated by 7.5% SDS-PAGE and transferred to polyvinylidene difluoride membranes (Millipore). Blots were stained with Ponceau S to confirm equal protein loading and efficient transfer. Blots were subsequently incubated with a 1:1000 dilution of an in-house-generated anti-ATP7A antibody [called 54-10 (7)] for 3 h followed by a 1:5000 dilution of an anti- α -tubulin antibody (catalog no. ab6046; Abcam) for 1 h. For detection of immunoreactive proteins, blots were incubated with an anti-IgG rabbit secondary antibody (catalog no. A120-101P; Bethyl Labs), followed by incubating blots with enhanced chemiluminescence reagent and then exposing them to X-ray film. The optical density of immunoreactive bands on film was quantified by using the digitizing software UN-SCAN-IT (Silk Scientific), and average pixel numbers were used for normalization and comparison. The intensity of ATP7A immunoreactive bands on film was normalized to the intensity of α -tubulin bands.

Reductase and oxidase activity assays

Reductase assay. Postconfluent IEC-6 cells cultured in 24-well plates were acclimated for 30 min at 37°C in Krebs-Ringer buffer. Cells were then incubated at 37°C for 90 min in 200 μ L Krebs-Ringer buffer containing 2 mmol/L nitroterazolium blue chloride (Sigma). After

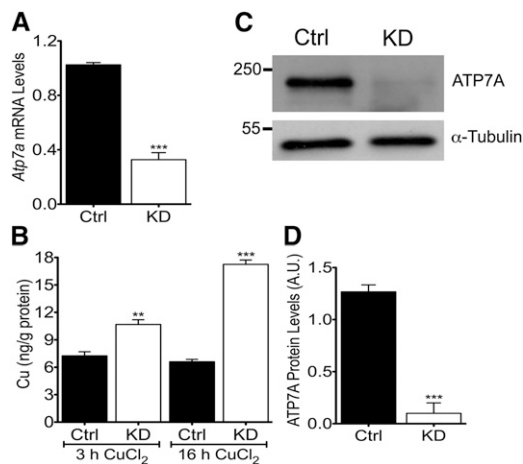


FIGURE 1 Copper efflux is impaired in *Atp7a* KD IEC-6 cells. IEC-6 cells transfected with *Atp7a*-specific, shRNA-expressing plasmids (KD) or a negative-control shRNA-expressing plasmid (Ctrl) were maintained in the presence of zeocin. *Atp7a* KD was confirmed at the mRNA (A) and protein (C, D) levels. *Atp7a* mRNA levels were normalized to cyclophilin expression (A). A representative blot is shown (C) along with quantitative data from all experiments (D). Confluent cells were loaded with CuCl_2 for 3 or 16 h, and intracellular copper concentrations were measured (B). Different from Ctrl: ** $P < 0.005$, *** $P < 0.001$ (Student's *t* test). Values are means \pm SDs; $n = 4$ independent experiments. *Atp7a*, Menkes copper-transporting ATPase; A.U., arbitrary units; Ctrl, control; IEC-6, rat intestinal epithelial; KD, knockdown; shRNA, short hairpin RNA.

incubation, cells were washed and photographed with an EVOS XL Core Cell Imaging system (Invitrogen). Color intensity was determined with the ImageJ color analysis program available online from the NIH (32).

Oxidase assay. Transferrin-coupled ferroxidase assay was performed with the use of 200 μg of cytosolic or 100 μg of membrane proteins isolated from control and *Atp7a* knockdown cells as described previously (33). Initial velocities from 30 to 120 s were obtained by following change in absorbance over time at 460 nm in a spectrophotometer (Implen), at room temperature. Blanks, lacking protein samples but otherwise identical, were run in parallel in each experiment to control for autooxidation of ferrous iron.

Statistical analysis

Results are expressed as means \pm SDs. All analyses were performed by using GraphPad Prism (version 5.0 for Windows). Student's *t* test was performed to compare 2 groups, and 1-factor ANOVA followed by Tukey's multiple comparisons test was used for comparing multiple groups. Relative FOX activity in IEC-6 cells was compared between experimental groups by 2-factor ANOVA followed by Bonferroni's multiple comparisons test.

Results

***Atp7a* knockdown impairs copper efflux.** *Atp7a* knockdown was confirmed at the mRNA, protein, and functional levels (Fig. 1). *Atp7a* mRNA levels were significantly reduced ($\sim 70\%$) in cells transfected with *Atp7a*-target shRNAs relative to cells transfected with the negative-control shRNA. This reduction in *Atp7a* mRNA expression paralleled ATP7A protein levels in the knockdown cells, which were reduced by $\sim 90\%$. Copper-loading experiments showed that intracellular copper concentrations were elevated to a greater extent in *Atp7a* knockdown cells compared with control cells (1.5-fold more copper at 3 h and 2.5-fold more at 16 h). Furthermore, under normal culture conditions, intracel-

lular iron and copper concentrations were unaffected by *Atp7a* knockdown (data not shown).

***Atp7a* knockdown increases transepithelial iron flux.** Postconfluent IEC-6 cell monolayers grown in bicameral cell culture inserts formed mature tight junctions and showed no evidence of leakiness. TEER was routinely $36\text{--}40 \Omega \times \text{cm}^2$ and phenol red transport was essentially zero (data not shown). ^{59}Fe accumulation in *Atp7a* knockdown cells (uptake) was significantly higher than in control cells ($\sim 50\%$ increase), and even more so after DFO treatment ($\sim 80\%$ increase) (Fig. 2). ^{59}Fe in cells was lower after DFO treatment in both cell lines ($\sim 65\%$ decrease). Additionally, transepithelial iron transport (transfer) was assessed by measuring ^{59}Fe accumulation in the basolateral chambers of cultured cells. *Atp7a* knockdown cells transferred more iron under control conditions ($\sim 33\%$ increase) and after DFO treatment ($\sim 70\%$ increase). Moreover, DFO treatment increased iron transfer across the basolateral membranes of both cell lines (control: $\sim 40\%$ increase; knockdown: $\sim 90\%$).

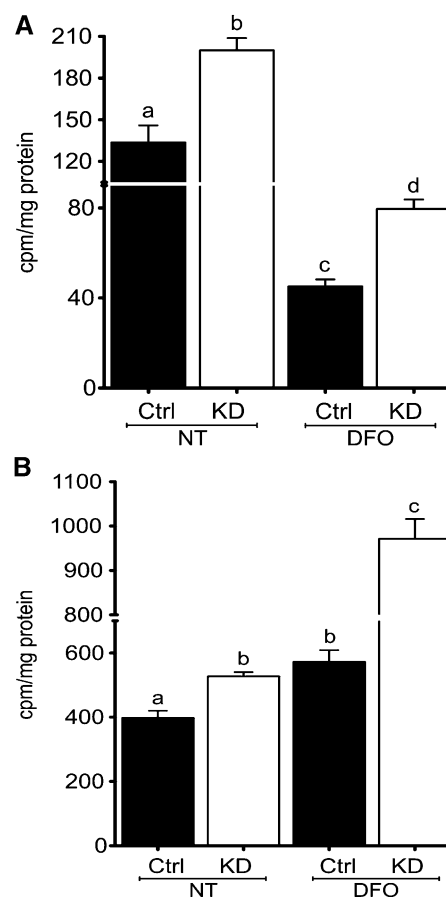


FIGURE 2 Transepithelial iron flux is enhanced in *Atp7a* KD IEC-6 cells. IEC-6 cells were grown for 8 d postconfluence on collagen-coated cell culture inserts, and TEER was measured to ensure integrity of monolayers. Subsequently, ^{59}Fe flux was determined. ^{59}Fe accumulation in cells (transport) with (DFO) and without (NT) iron chelation (A). ^{59}Fe flux from cells to the basolateral chamber (transfer) (B). Uptake and transfer of ^{59}Fe were normalized to protein content of cell extracts. Labeled means without a common letter differ, $P < 0.05$ (1-factor ANOVA). Values are means \pm SDs; $n = 5$ independent experiments. *Atp7a*, Menkes copper-transporting ATPase; Ctrl, control; DFO, deferoxamine; IEC-6, rat intestinal epithelial; KD, knockdown; NT, no treatment; TEER, transepithelial electrical resistance.

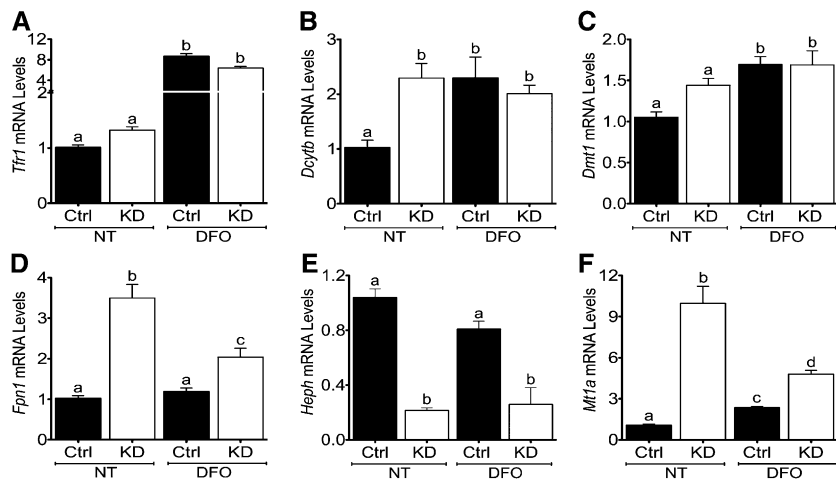


FIGURE 3 Expression of iron and copper homeostasis-related genes is altered in *Atp7a* KD IEC-6 cells (A–F). Ctrl or *Atp7a* KD IEC-6 cells were cultured for 8 d postconfluence and then qRT-PCR was used to quantify gene expression levels. Cells were either cultured under normal conditions (NT) or treated with an iron chelator (DFO) for 24 h. Labeled means without a common letter differ, $P < 0.05$ (1-factor ANOVA). Values are means \pm SDs; $n = 8$ for all groups and treatments. *Atp7a*, Menkes copper-transporting ATPase; Ctrl, control; *Dcytb*, duodenal cytochrome b; DFO, deferoxamine; *Dmt1*, divalent metal transporter 1; *Fpn1*, ferroportin 1; *Heph*, hephaestin; IEC-6, rat intestinal epithelial; KD, knockdown; *Mt1a*, metallothionein 1a; NT, no treatment; *Tfr1*, transferrin receptor 1.

Atp7a knockdown alters expression of iron and copper homeostasis-related genes. Gene expression was assessed in differentiated control and *Atp7a* knockdown IEC-6 cells (Fig. 3). Transferrin receptor 1 (*Tfr1*) mRNA expression was significantly induced in both control and *Atp7a* knockdown cells after DFO treatment. Unexpectedly, *Dcytb* (2.3-fold), *Fpn1* (3.5-fold), and metallothionein 1a (*Mt1a*; 10-fold) mRNA expression was increased in knockdown cells. *Fpn1* (1.7-fold) and *Mt1a* (2-fold) were also induced in knockdown cells with DFO treatment, but *Dcytb* expression was not different in control versus knockdown cells under DFO-exposed conditions. Conversely, *Atp7a* knockdown reduced *Heph* mRNA expression (~80%) in control and DFO-treated cells. *Atp7a* knockdown did not, however, significantly affect divalent metal transporter 1 (*Dmt1*) mRNA expression, but DFO treatment induced *Dmt1* expression in control and knockdown cells (~1.7-fold). Furthermore, *Atp7a* knockdown and DFO treatment did not affect expression of copper transporter 1 (*Ctrl*) or ferritin, and Wilsons copper-transporting ATPase (*Atp7b*) mRNA was not detected in either cell line under control or iron-deprived conditions (data not shown).

Ferrireductase activity increases in *Atp7a* knockdown IEC-6 cells. IEC-6 cells were incubated with 2 mmol/L nitro-tetrazolium blue chloride; the intensity of blue staining correlates with reductase activity. *Atp7a* knockdown cells had more intense blue color (~15% higher) than control cells cultured under identical conditions (Fig. 4).

Membrane and cytosolic FOX activity is partially attenuated by Atp7a knockdown. Membrane and cytosolic proteins were isolated from control and *Atp7a* knockdown IEC-6 cells by a validated protocol (31,33). Before experimentation, relative purity was nonetheless assessed by Western blotting (Fig. 5). Immunoreactive ATP7A protein was only detected in membrane fractions, and as expected, protein expression levels were reduced in *Atp7a* target shRNA-transfected (knockdown) IEC-6 cells. FOX activity was detected in membrane and cytosolic fractions isolated from the IEC-6 cells. In membrane fractions, FOX activity decreased by 30–50% in *Atp7a* knockdown cells. Similar results were noted in cytosolic fractions, with *Atp7a* knockdown partially attenuating activity (~25% reduction).

Fpn1 gene transcription rate increases in *Atp7a* knockdown IEC-6 cells. To determine whether increases in *Dcytb* and

Fpn1 mRNA expression related to changes in transcription rates, further experiments were performed. *Dcytb* and *Fpn1* mRNA expression increased in *Atp7a* knockdown cells (as expected), whereas actinomycin D treatment decreased mRNA expression of both genes in both cell lines (Fig. 6). The increase in expression in the knockdown cells, however, was maintained for *Dcytb* in the presence of actinomycin D, whereas *Fpn1* expression was no longer increased. Furthermore, *Dcytb* hnRNA levels increased to a lesser extent (1.7-fold) than mRNA (3.1-fold), whereas *Fpn1* mRNA (2.3-fold) and hnRNA (2.5-fold) increased to a similar extent in *Atp7a* knockdown cells compared with control cells. Because *Dcytb* mRNA increased more dramatically than hnRNA ($P = 0.016$), transcriptional and posttranscriptional mechanisms are likely involved, whereas the very similar alterations in *Fpn1* mRNA and hnRNA ($P = 0.47$) suggest that the induction is transcriptionally mediated.

Discussion

Atp7a mRNA expression was induced in the duodenal epithelium during iron deficiency, mirroring the expression patterns of *Dcytb*, *Dmt1*, and metallothionein 1 and 2 (6). This initial observation piqued our interest in the influence of copper on iron homeostasis, a subject that has been considered by many investigators (14,34,35). It was subsequently shown that *Atp7a* expression is coregulated along with *Dcytb*, *Dmt1*, and *Fpn1* by a hypoxia-inducible transcription factor, HIF2 α (8). This observation, when considered in the context of the frequently observed increases in copper concentrations in some tissues during iron deprivation, supports the possibility that *Atp7a* is a molecular link between iron and copper homeostasis. Because ATP7A is the rate-limiting step in body copper acquisition (17), and it can influence copper concentrations in enterocytes and hepatocytes, it is certainly properly positioned to influence iron metabolism. The current investigation was thus designed to directly elucidate the influence of ATP7A function on iron homeostasis in enterocytes, by silencing *Atp7a* expression in an accepted model of the mammalian intestinal epithelium.

ATP7A has dual functions in enterocytes, including pumping copper into the TGN where cuproenzyme synthesis occurs and exporting copper across the basolateral membrane under conditions of copper excess (36). *Atp7a* knockdown IEC-6 cells accumulated more copper than control cells when acutely exposed to excess copper in the medium, reflecting perturbed ATP7A export function. When grown in regular medium, intracellular

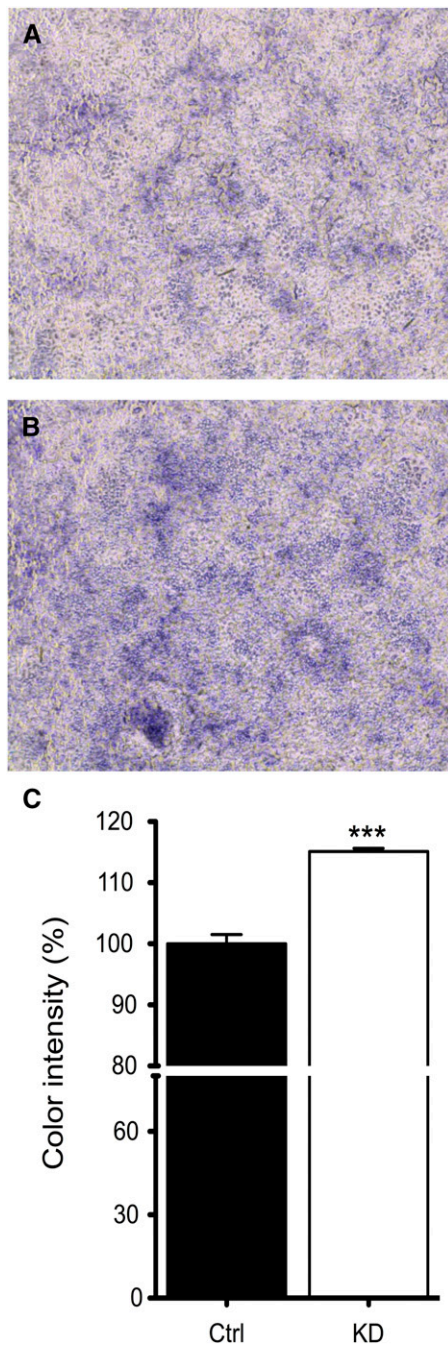


FIGURE 4 Cell surface ferrireductase activity increases in *Atp7a* KD IEC-6 cells. Ctrl or *Atp7a* KD IEC-6 cells were cultured for 8 d postconfluence and then incubated with 2 mmol/L nitroterazolium blue chloride. Color intensity was determined by the ImageJ color analysis program (NIH). Representative pictures are shown from control (A) or knockdown (B) cells. Color intensity quantification from all experiments (C). ***Different from Ctrl, $P < 0.001$ (Student's t test). Values are means \pm SDs; $n = 5$ independent experiments. *Atp7a*, Menkes copper-transporting ATPase; Ctrl, control; IEC-6, rat intestinal epithelial; KD, knockdown.

copper concentrations were not different when comparing knockdown with control cells. Perturbations in intracellular copper homeostasis were, however, probable in knockdown cells, because impaired copper transport into the TGN likely alters intracellular copper distribution (and impairs cuproenzyme synthesis). Induction of *Mt1a* mRNA expression (~ 10 -fold) also supports this possibility, because *Mt* is induced by

copper (37). This is exemplified in Menkes disease, in which dysfunctional ATP7A results in copper accumulation in enterocytes, resulting in induction of *MT*, which stores (detoxifies) excess copper until it can be eliminated by exfoliation of epithelial cells (38). Induction of *Mt* could also result secondarily from production of ROS (39). Because copper is redox active, intracellular copper accumulation could produce ROS. In *Atp7a* knockdown cells, *Mt* induction is most likely a result of copper accumulation in one or more intracellular compartments. As would be predicted then, *Atp7a* silencing perturbs intracellular copper homeostasis.

Atp7a expression is induced during iron deficiency in the rat intestine, and one might thus postulate that ATP7A function promotes iron transport. This is a logical prediction because many genes encoding proteins involved in iron transport are upregulated during iron deprivation. Enhanced ATP7A function could potentiate biosynthesis of the active (copper-containing) form of HEPH, if HEPH is produced in the TGN similar to other

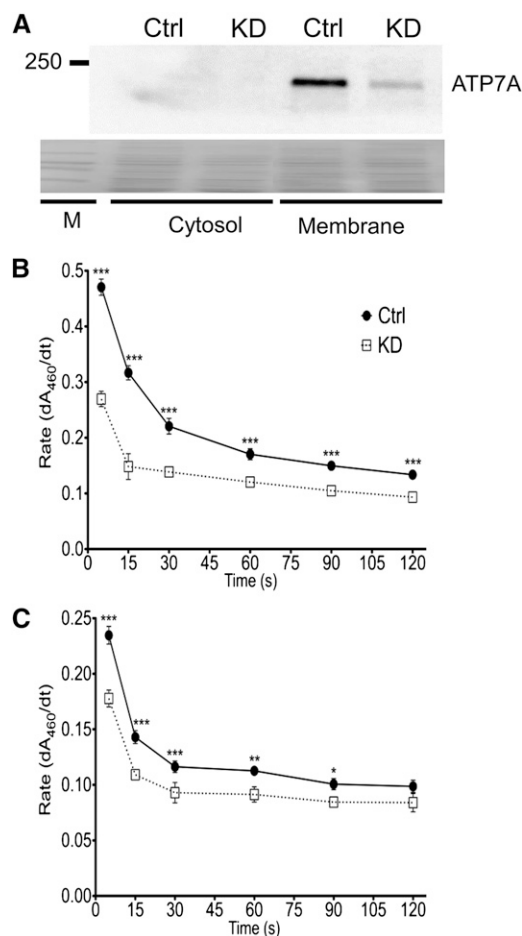


FIGURE 5 Membrane and cytosolic FOX activity is partially attenuated in *Atp7a* KD IEC-6 cells. Membrane and cytosolic proteins were isolated from postconfluent control and *Atp7a* KD cells. Western blot analysis of protein fractions using a well-established anti-*Atp7a* antibody (A). Blot shown is representative of 3 independent experiments with similar results. Stained proteins on the blot (shown below) exemplify similar protein loading and efficient transfer onto the membrane. FOX activity by a transferrin-coupled assay is shown in membrane (B) and cytosolic (C) fractions. Different from Ctrl: * $P < 0.05$, ** $P < 0.005$, *** $P < 0.001$ (2-factor ANOVA). Values are means \pm SDs; $n = 6$ per group and treatment. *Atp7a*, Menkes copper-transporting ATPase; Ctrl, control; dA₄₆₀/dt, change in absorbance over time; FOX, ferroxidase; IEC-6, rat intestinal epithelial; KD, knockdown; M, marker.

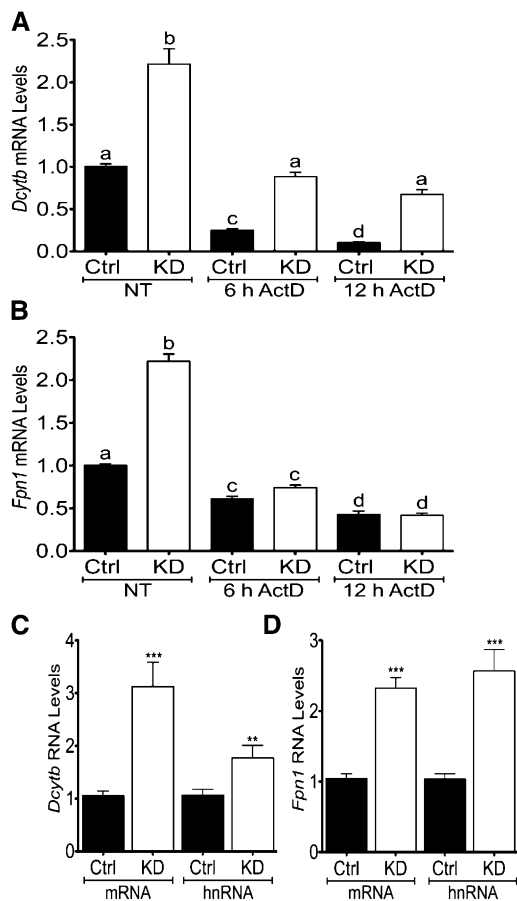


FIGURE 6 *Fpn1* gene transcription rate increases in *Atp7a* KD IEC-6 cells. Postconfluent control and *Atp7a* KD IEC-6 cells were cultured under normal conditions (NT) or treated with a transcriptional inhibitor (ActD) for 6 or 12 h, and *Dcytb* (A) and *Fpn1* (B) mRNA expression levels were determined by qRT-PCR. mRNA expression levels of both genes were also directly compared with hnRNA levels (C, D). Labeled means without a common letter differ, $P < 0.05$ (1-factor ANOVA). Different from Ctrl: ** $P < 0.005$, *** $P < 0.001$ (Student's *t* test). Values are means \pm SDs; $n = 6$ for all groups and treatments. ActD, actinomycin D; *Atp7a*, Menkes copper-transporting ATPase; Ctrl, control; *Dcytb*, duodenal cytochrome b; *Fpn1*, ferroportin 1; hnRNA, heteronuclear RNA; IEC-6, rat intestinal epithelial; KD, knockdown; NT, no treatment.

cuproenzymes (which is unknown). Such a possibility is supported by the fact that an analogous copper-transporting ATPase (*Atp7b*) expressed in hepatocytes pumps copper into the TGN for production of CP (40), another copper-dependent FOX involved in iron homeostasis. It was in fact hypothesized that CP activity increases during iron deficiency due to increased cellular copper content leading to enhanced metallation and production of the *holo* (active) form of the enzyme (11,41). If the postulate that ATP7A activity promotes iron absorption is indeed correct, then lack of expression would be expected to decrease iron transport. In the current study, however, *Atp7a* silencing unexpectedly had the opposite effect: it increased transepithelial iron flux.

Iron uptake across the apical membrane and export across the basolateral membrane were enhanced in *Atp7a* knockdown cells. Apical iron uptake is influenced by dietary reducing agents (e.g., ascorbate) and by a cell surface ferrireductase (probably DCYTB), which provide ferrous iron ions for transport into cells by DMT1. Increased iron uptake into *Atp7a* knockdown cells was noted in the absence of exogenous reducing agents. This was associated with increased *Dcytb* mRNA expression and cell

surface ferrireductase activity. *Dmt1* mRNA expression, however, was not altered in this setting, probably because intracellular iron concentrations were not altered in *Atp7a* knockdown cells and cells were not hypoxic. *Dmt1* is principally regulated at the level of mRNA expression, via transcriptional and post-transcriptional mechanisms. *Dmt1* mRNA levels increase when intracellular iron is low, via stabilization of a *Dmt1* transcript variant by interaction with iron-regulatory proteins (42). Under conditions of tissue hypoxia, the *Dmt1* gene is transactivated by a hypoxia-inducible transcription factor (HIF2 α) (4). Enhanced ferrireductase activity thus likely mediates the increase in iron uptake into *Atp7a* knockdown cells.

Iron efflux across the basolateral surface of enterocytes involves transport by FPN1, coupled to iron oxidation by a ferroxidase (probably membrane-bound HEPH), allowing ferric iron binding to transferrin in the interstitial fluids within the lamina propria of duodenal villi. Enhanced iron efflux from *Atp7a* knockdown cells was associated with induction of *Fpn1* mRNA expression. Unexpectedly however, *Heph* mRNA expression was significantly reduced (by $\sim 80\%$) and membrane FOX activity was diminished (by $\sim 50\%$). Reduced FOX activity could result from decreased *Heph* expression and/or defective protein biosynthesis due to a lack of copper in the TGN (if HEPH is indeed synthesized there). Why reduced membrane FOX activity did not inhibit iron efflux is unclear. Studies in mice expressing a mutant HEPH protein with reduced activity (*sla* mice) showed that HEPH contributes to iron flux during periods of rapid postnatal growth, but HEPH is not necessary for iron absorption in adult mice (43). Moreover, a soluble, cytosolic FOX was recently discovered (31), which could complement HEPH function. A soluble form of HEPH was also recently documented in enterocyte cytosolic fractions (32). *Atp7a* knockdown cells retained $\sim 50\%$ of membrane FOX activity, and had robust cytosolic FOX activity (75% of control cells). Therefore, given that more than one enterocyte FOX may exist, HEPH activity may not be rate-limiting for iron transport, even under conditions when transepithelial iron flux increases.

As detailed above, increased iron flux in *Atp7a* knockdown cells is likely explained by enhanced expression and activity of an apical surface ferrireductase (likely DCYTB) and the basolateral iron exporter (FPN1). Further experiments were thus undertaken to elucidate the molecular mechanism by which *Atp7a* silencing resulted in an increase of *Dcytb* and *Fpn1* mRNA levels. Use of a transcriptional inhibitor and quantification of hnRNA levels demonstrated that *Fpn1* induction was transcriptionally mediated, whereas the mechanism of *Dcytb* induction was less clear, perhaps involving transcriptional and posttranscriptional mechanisms. Transcriptional regulation of the *Fpn1* gene in intestinal epithelial cells, unrelated to hypoxia (44), has not been previously reported.

The effect of *Atp7a* knockdown on iron flux was even more dramatic in cells treated with an iron chelator. Under these conditions, ^{59}Fe concentrations were reduced in *Atp7a* knockdown and control cells, whereas ^{59}Fe transferred to the basolateral chamber increased in both cell lines. DFO treatment increased *Tfr1* expression, indicative of intracellular iron depletion (45). In DFO-treated cells, *Dmt1* expression increased similarly in both cell lines, consistent with decreased intracellular iron. *Heph* mRNA expression was reduced in DFO-treated *Atp7a* knockdown cells to a similar extent as in untreated cells. Induction of *Fpn1* and *Mt1a* was noted in DFO-treated *Atp7a* knockdown cells, similar to cells cultured under control conditions. From these observations, it is difficult to predict the mechanism by which *Atp7a* knockdown further increases transepithelial iron

flux in iron-deprived cells, but nonetheless these experiments provide further evidence that ATP7A function influences enterocyte iron homeostasis.

The influence of copper on iron absorption was previously investigated in the Caco-2 cell model (28). Cells chronically exposed to excess copper had a 10-fold increase in intracellular copper concentrations and transported more iron, which correlated with increased expression of *Dmt1*, *Fpn1*, and *Heph* mRNA. A model was proposed in which copper depletes intracellular iron, thus indirectly enhancing iron transport. The observations of the current study, although also supporting a role for copper in iron transport, differ in notable ways. First, under normal culture conditions in which iron transport studies were performed, no changes in intracellular copper content were noted in *Atp7a* knockdown cells (by atomic absorption spectroscopy). Second, intracellular iron concentrations were not different in *Atp7a* knockdown versus control cells and *Tfr1* mRNA expression was not altered (as a sensitive marker of intracellular iron). This may be due to the fact that iron uptake and efflux were both stimulated in knockdown cells (Fig. 2). Moreover, enhanced iron transport occurred when *Heph* mRNA levels and FOX activity decreased (unlike in the aforementioned study). The current results cannot thus be explained by intracellular copper accumulation causing depletion of intracellular iron, demonstrating a distinct regulatory mechanism mediating increased iron flux in *Atp7a* knockdown cells.

This study provides further support of a functional role for the ATP7A copper transporter in intestinal iron homeostasis. Decreased ATP7A function may alter intracellular copper trafficking or distribution, which, in turn, stimulates iron transport. How *Atp7a* silencing increases *Dcytb* expression and activity, and activates *Fpn1* transcription, is currently unknown. These observations are difficult to reconcile with the fact that *Atp7a* expression is induced in rat duodenum during iron deficiency. It is, however, important to emphasize that increased *Atp7a* expression in rat duodenal enterocytes is accompanied by induction of *Mt* (and increased mucosal copper concentrations), whereas *Atp7a* knockdown in iron-deprived IEC-6 cells also induces metallothionein (likely indicative of altered intracellular copper homeostasis). Moreover, a recent study in Brindled mice expressing a mutant ATP7A protein showed that copper accumulates in enterocytes during iron deprivation, which may have positively influenced iron absorption (29). The unanticipated finding from this investigation is that upregulation of *Atp7a* in vivo and knockdown of *Atp7a* in vitro may have similar effects on intracellular copper pools, perhaps leading to a similar biologic response that promotes iron absorption. The common theme that emerges from this and previous investigations is that alterations in ATP7A function lead to perturbed intracellular copper homeostasis, which influences iron transport. The identification of ATP7A as a molecular link between iron and copper metabolism provides mechanistic insight into longstanding hypotheses about the influence of copper on intestinal iron absorption (14).

Acknowledgments

S.G. and J.F.C. designed the research, analyzed the data, and wrote the manuscript; S.G. conducted the research and performed statistical analysis; and J.F.C. had primary responsibility for final content. Both authors read and approved the final manuscript.

Literature Cited

1. Fleming RE, Ponka P. Iron overload in human disease. *N Engl J Med*. 2012;366:348–59.
2. Ganz T, Nemeth E. Iron imports. IV. Hepcidin and regulation of body iron metabolism. *Am J Physiol Gastrointest Liver Physiol*. 2006;290:G199–203.

3. Hu Z, Gulec S, Collins JF. Cross-species comparison of genomewide gene expression profiles reveals induction of hypoxia-inducible factor-responsive genes in iron-deprived intestinal epithelial cells. *Am J Physiol Cell Physiol*. 2010;299:C930–8.
4. Shah YM, Matsubara T, Ito S, Yim SH, Gonzalez FJ. Intestinal hypoxia-inducible transcription factors are essential for iron absorption following iron deficiency. *Cell Metab*. 2009;9:152–64.
5. Mastrogiannaki M, Matak P, Keith B, Simon MC, Vaulont S, Peyssonnaud C. HIF-2alpha, but not HIF-1alpha, promotes iron absorption in mice. *J Clin Invest*. 2009;119:1159–66.
6. Collins JF, Franck CA, Kowdley KV, Ghishan FK. Identification of differentially expressed genes in response to dietary iron deprivation in rat duodenum. *Am J Physiol Gastrointest Liver Physiol*. 2005;288:G964–71.
7. Ravia JJ, Stephen RM, Ghishan FK, Collins JF. Menkes Copper ATPase (Atp7a) is a novel metal-responsive gene in rat duodenum, and immunoreactive protein is present on brush-border and basolateral membrane domains. *J Biol Chem*. 2005;280:36221–7.
8. Xie L, Collins JF. Transcriptional regulation of the Menkes copper ATPase (Atp7a) gene by hypoxia inducible factor (Hif2a) in intestinal epithelial cells. *Am J Physiol Cell Physiol*. 2011;300:C1298–305.
9. Sourkes TL, Lloyd K, Birnbaum H. Inverse relationship of hepatic copper and iron concentrations in rats fed deficient diets. *Can J Biochem*. 1968;46:267–71.
10. Cartwright GE, Huguley CM Jr, Ashenbrucker H, Fay J, Wintrobe WW. Studies on free erythrocyte protoporphyrin, plasma iron and plasma copper in normal and anemic subjects. *Blood*. 1948;3:501–25.
11. Ranganathan PN, Lu Y, Jiang L, Kim C, Collins JF. Serum ceruloplasmin protein expression and activity increases in iron-deficient rats and is further enhanced by higher dietary copper intake. *Blood*. 2011;118:3146–53.
12. El-Shobaki FA, Rummel W. Binding of copper to mucosal transferrin and inhibition of intestinal iron absorption in rats. *Res Exp Med (Berl)*. 1979;174:187–95.
13. Ece A, Uyanik BS, Iscan A, Ertan P, Yigitoglu MR. Increased serum copper and decreased serum zinc levels in children with iron deficiency anemia. *Biol Trace Elem Res*. 1997;59:31–9.
14. Fox PL. The copper-iron chronicles: the story of an intimate relationship. *Biometals*. 2003;16:9–40.
15. Gitlin JD. Aceruloplasminemia. *Pediatr Res*. 1998;44:271–6.
16. Chen H, Su T, Attieh ZK, Fox TC, McKie AT, Anderson GJ, Vulpe CD. Systemic regulation of hephaestin and Ireg1 revealed in studies of genetic and nutritional iron deficiency. *Blood*. 2003;102:1893–9.
17. Vulpe C, Levinson B, Whitney S, Packman S, Gitschier J. Isolation of a candidate gene for Menkes disease and evidence that it encodes a copper-transporting ATPase. *Nat Genet*. 1993;3:7–13.
18. Thomas C, Oates PS. IEC-6 cells are an appropriate model of intestinal iron absorption in rats. *J Nutr*. 2002;132:680–7.
19. Carroll KM, Wong TT, Drabik DL, Chang EB. Differentiation of rat small intestinal epithelial cells by extracellular matrix. *Am J Physiol Gastrointest Liver Physiol*. 1988;254:G355–60.
20. Oates PS, Thomas C. Augmented internalisation of ferroportin to late endosomes impairs iron uptake by enterocyte-like IEC-6 cells. *Pflugers Arch*. 2005;450:317–25.
21. Thomas C, Oates PS. Differences in the uptake of iron from Fe(II) ascorbate and Fe(III) citrate by IEC-6 cells and the involvement of ferroportin/IREG-1/MTP-1/SLC40A1. *Pflugers Arch*. 2004;448:431–7.
22. Thomas C, Oates PS. Ferroportin/IREG-1/MTP-1/SLC40A1 modulates the uptake of iron at the apical membrane of enterocytes. *Gut*. 2004;53:44–9.
23. Wood SR, Zhao Q, Smith LH, Daniels CK. Altered morphology in cultured rat intestinal epithelial IEC-6 cells is associated with alkaline phosphatase expression. *Tissue Cell*. 2003;35:47–58.
24. Bastian SE, Walton PE, Ballard FJ, Belford DA. Transport of IGF-I across epithelial cell monolayers. *J Endocrinol*. 1999;162:361–9.
25. Puthia MK, Sio SW, Lu J, Tan KS. Blastocystis ratti induces contact-independent apoptosis, F-actin rearrangement, and barrier function disruption in IEC-6 cells. *Infect Immun*. 2006;74:4114–23.
26. Forsythe RM, Xu DZ, Lu Q, Deitch EA. Lipopolysaccharide-induced enterocyte-derived nitric oxide induces intestinal monolayer permeability in an autocrine fashion. *Shock*. 2002;17:180–4.
27. Linder MC, Zerounian NR, Moriya M, Malpe R. Iron and copper homeostasis and intestinal absorption using the Caco2 cell model. *Biometals*. 2003;16:145–60.

28. Han O, Wessling-Resnick M. Copper repletion enhances apical iron uptake and transepithelial iron transport by Caco-2 cells. *Am J Physiol Gastrointest Liver Physiol*. 2002;282:G527–33.
29. Gulec S, Collins JF. Investigation of iron metabolism in mice expressing a mutant Menke's copper transporting ATPase (Atp7a) protein with diminished activity (Brindled; Mo (Br) (*ly*)). *PLoS ONE*. 2013;8:e66010.
30. Collins JF, Hua P, Lu Y, Ranganathan PN. Alternative splicing of the Menkes copper ATPase (Atp7a) transcript in the rat intestinal epithelium. *Am J Physiol Gastrointest Liver Physiol*. 2009;297:G695–707.
31. Ranganathan PN, Lu Y, Fuqua BK, Collins JF. Discovery of a cytosolic/soluble ferroxidase in rodent enterocytes. *Proc Natl Acad Sci USA*. 2012;109:3564–9.
32. Schneider CA, Rasband WS, Eliceiri KW. NIH Image to ImageJ: 25 years of image analysis. *Nat Meth*. 2012;9:671–5.
33. Ranganathan PN, Lu Y, Fuqua BK, Collins JF. Immunoreactive hephaestin and ferroxidase activity are present in the cytosolic fraction of rat enterocytes. *Biometals*. 2012;25:687–95.
34. Klevay LM. Copper as a supplement to iron for hemoglobin building in the rat (Hart et al., 1928). *J Nutr*. 1997;127 Suppl:1034S–6S.
35. Chase MS, Gubler CJ, Cartwright GE, Wintrobe MM. Studies on copper metabolism. IV. The influence of copper on the absorption of iron. *J Biol Chem*. 1952;199:757–63.
36. Petris MJ, Mercer JF, Culvenor JG, Lockhart P, Gleeson PA, Camakaris J. Ligand-regulated transport of the Menkes copper P-type ATPase efflux pump from the Golgi apparatus to the plasma membrane: a novel mechanism of regulated trafficking. *EMBO J*. 1996;15:6084–95.
37. Heuchel R, Radtke F, Georgiev O, Stark G, Aguet M, Schaffner W. The transcription factor MTF-1 is essential for basal and heavy metal-induced metallothionein gene expression. *EMBO J*. 1994;13:2870–5.
38. Kelly EJ, Palmiter RD. A murine model of Menkes disease reveals a physiological function of metallothionein. *Nat Genet*. 1996;13:219–22.
39. Vašák M, Meloni G. Chemistry and biology of mammalian metallothioneins. *J Biol Inorg Chem*. 2011;16:1067–78.
40. Terada K, Nakako T, Yang XL, Iida M, Aiba N, Minamiya Y, Nakai M, Sakaki T, Miura N, Sugiyama T. Restoration of holoceruloplasmin synthesis in LEC rat after infusion of recombinant adenovirus bearing WND cDNA. *J Biol Chem*. 1998;273:1815–20.
41. Sternlieb I, Morell AG, Tucker WD, Greene MW, Scheinberg IH. The incorporation of copper into ceruloplasmin in vivo: studies with copper and copper. *J Clin Invest*. 1961;40:1834–40.
42. Galy B, Ferring-Appel D, Kaden S, Grone HJ, Hentze MW. Iron regulatory proteins are essential for intestinal function and control key iron absorption molecules in the duodenum. *Cell Metab*. 2008;7:79–85.
43. Vulpe CD, Kuo YM, Murphy TL, Cowley L, Askwith C, Libina N, Gitschier J, Anderson GJ. Hephaestin, a ceruloplasmin homologue implicated in intestinal iron transport, is defective in the sla mouse. *Nat Genet*. 1999;21:195–9.
44. Taylor M, Qu A, Anderson ER, Matsubara T, Martin A, Gonzalez FJ, Shah YM. Hypoxia-inducible factor-2alpha mediates the adaptive increase of intestinal ferroportin during iron deficiency in mice. *Gastroenterology*. 2011;140:2044–55.
45. Casey JL, Hentze MW, Koeller DM, Caughman SW, Rouault TA, Klausner RD, Harford JB. Iron-responsive elements: regulatory RNA sequences that control mRNA levels and translation. *Science*. 1988;240:924–8.